UCRL-JRNL-203888

Low Dose Radiation Hypersensitivity is Caused by p53-dependent Apoptosis

L. Enns, K.T. Bogen, J. Wizniak, A.D. Murtha, M. Weinfeld

September 4, 2004

Accepted for publication in *Molecular Cancer Research*

Work supported in part by the
USDOE Low Dose Radiation Research Program

Low Dose Radiation Hypersensitivity is Associated with p53-dependent Apoptosis

Louise Enns[1], Kenneth T. Bogen[2], Juanita Wizniak[1], Albert D. Murtha[1], Michael Weinfeld[1,3]

[1]Cross Cancer Institute, 11560 University Ave, Edmonton, Alberta, T6G 1Z2, Canada

[2]Environmental Science Division (L-396), Lawrence Livermore National Laboratory, 7000 East Ave., Livermore, CA 94550-9900, USA

Running title: Apoptosis and low dose radiation hypersensitivity

Keywords: apoptosis, low-dose radiation, annexin V, caspase-3, gel microdrops, survival

[3]Corresponding author: Tel.: 780 432 8438; fax: 780 432 8428;

E-mail: michaelw@cancerboard.ab.ca

Funding for this project was provided in part under the auspices of the U.S. Department of Energy by the University of California, Lawrence Livermore National Laboratory under contract No. W-7405-Eng-48, the National Cancer Institute (Canada) grant No. 013104 and the Alberta Cancer Board Bridge and Pilot grant No. R-418, and the DOE Low Dose Radiation Research Program.

Abstract

Exposure to environmental radiation and the application of new clinical modalities, such as radioimmunotherapy, have heightened the need to understand cellular responses to low dose and low-dose rate ionizing radiation. Many tumor cell lines have been observed to exhibit a hypersensitivity to radiation doses below 50 cGy, which manifests as a significant deviation from the clonogenic survival response predicted by a linear-quadratic fit to higher doses. However, the underlying processes for this phenomenon remain unclear. Using a gel microdrop/flow cytometry assay to monitor single cell proliferation at early times post irradiation, we examined the response of human A549 lung carcinoma, T98G glioma and MCF7 breast carcinoma cell lines exposed to gamma radiation doses from 0 to 200 cGy delivered at 0.18 and 22 cGy/min. The A549 and T98G cells, but not MCF7 cells, showed the marked hypersensitivity at doses <50 cGy. To further characterize the low-dose hypersensitivity, we examined the influence of low-dose radiation on cell cycle status and apoptosis by assays for active caspase-3 and phosphatidylserine translocation (annexin-V binding). We observed that caspase-3 activation and annexin-V binding mirrored the proliferation curves for the cell lines. Furthermore, the low-dose hypersensitivity and annexin-V binding to irradiated A549 and T98G cells were eliminated by treating the cells with pifithrin, an inhibitor of p53**.** When p53-inactive cell lines (2800T skin fibroblasts and HCT116 colorectal carcinoma cells) were examined for similar patterns, we found that there was no HRS and apoptosis was not detectable by annexin-V or caspase-3 assays**.** Our data therefore suggest that low-dose hypersensitivity is associated with p53-dependent apoptosis.

Introduction

The effects of low dose and low-dose rate ionizing radiation continue to be of interest because of the potential dangers posed by exposure to environmental and occupational sources of radiation (1) and because of the potential clinical benefits of radioimmunotherapy (2). Seminal studies by Joiner, Marples and co-workers (3,4) and Wouters and Skarsgard (5-7) revealed that many human tumor cell lines exhibit a low-dose hypersensitivity to radiation (termed HRS for hyperradiosensitivity). This is usually manifest below ~0.5 Gy as a clear deviation from the standard linear quadratic cell survival response extrapolated from higher doses back to 0 Gy. It is accompanied by an increase in radioresistance at doses between ~50 and 100 cGy (termed IRR for increased radioresistance).

Several explanations have been proposed for the HRS/IRR phenomenon (reviewed in references 8-10). HRS may represent a subpopulation of cells that are hypersensitive due possibly to a cell cycle factor or more remotely a genetic predisposition. It has been reasoned that if there is a hypersensitive phase of the cell cycle, continuous low-dose rate irradiation should be more effective at inducing HRS because cells would be eliminated as they moved through this phase (6). Earlier models for IRR, on the other hand, assumed that the population of cells is uniformly hypersensitive to start with and becomes resistant as a function of dose due to some protective mechanism, such as induction of DNA repair (11) or down-regulation of programmed cell death (6). Recently, it was shown that cells in G_2 phase display elevated HRS in comparison to cells in G_1 or S phases (12) and a model has emerged for IRR that involves the activation of a G_2 phase checkpoint (13) which promotes DNA repair and cell survival (9,10). To date, however, the mode of death for those cells that die at the low doses has still not been ascertained.

HRS/IRR has been observed in many cell lines by a variety of different assays for cell killing and cell proliferation, including conventional colony-forming assays (14), and newer micro imaging methods (15). We recently reported on the application of a gel microdrop protocol (GMD) (16,17) to a low-dose radiation response of human A549 cells (18). The principal advantage of this approach is that it allows direct assessment of proliferation of the irradiated cells. By comparison, the colony-forming assay cannot distinguish between early and late effects that may lead to a reduction in the eventual number of colonies derived from the irradiated population. Other advantages of the GMD approach are that results can be obtained within 4-5 days after irradiation and, since it is a flow cytometric technique, up to $2x10^4$ single cells or microcolonies in GMDs can be analyzed at each dose.

Here we describe a detailed study of the low dose response of three human cell lines, A549 and T98G cells, which have previously been shown to display HRS/IRR (6, 19), and MCF7 cells, which do not (Michael Joiner, personal communication). Two dose rates differing by two orders of magnitude were used to examine the potential influence of low-dose rate radiation. The GMD assay confirmed the early nature of the HRS response and so we sought to further characterize the HRS response by analyzing the effects of low dose irradiation of these cell lines, in particular influences on cell cycle distribution and modes of cell death. An early clue that HRS may be due to an apoptotic response lay in the fact that MCF7 cells lack caspase-3 activation (20), a key caspase for a p53-dependent apoptotic pathway. By further examination of apoptosis with markers for translocation of phosphatidylserine and caspase-3 cleavage and p53 dependence using pifithrin, a specific inhibitor of p53, we found that HRS reflects a p53-dependent apoptotic

pathway. This finding was strengthened by an analysis of HRS in $p53^{+/+}$ and $p53^{-/-}$ HCT116 cells and in three human fibroblast lines including a p53-inactive fibroblast line.

Materials and Methods

Reagents

Cell culture reagents included Dulbecco's minimal essential medium/Ham's F12 nutrient mix (DMEM/F12), Ham's balanced salt solution (HBSS), L-glutamine, trypsin and fetal calf serum (FCS) (all from Invitrogen/GIBCO, Grand Island, NY). General cell culture-grade chemicals were obtained from Sigma Chemicals (St. Louis, MO). Anti-mouse and anti-rabbit secondary antibodies (HRP-conjugated) were supplied by Santa Cruz Biotechnology Inc (Santa Cruz, CA) and cyclin B1 and cdk1 were from BD Biosciences (Mississauga, ON). An enhanced chemiluminescence detection kit was purchased from Amersham (Baie d'Urfe, PQ) as was the Kodak X-OMAT AR autoradiographic film. Annexin V-FITC and a caspase-3 detection kit were obtained from BD Biosciences. Pifithrin was purchased from Biomol (Plymouth Meeting, PA).

Cell culture

Human A549 lung adenocarcinoma cells, T98G glioma cells and MCF7 breast carcinoma cells were obtained from the American Type Culture Collection (Rockland, MD); normal human fibroblasts, CRL2522 and GM38, were purchased from the NIGMS Human Genetic Cell Repository (Camden, NJ); the $p53^{-/-}$ human colorectal carcinoma cell line, HCT116 #2, and its $p53^{+/+}$ parent cell line, HCT116 #8, were kindly supplied by Dr. Bert Vogelstein (The Howard Hughes Medical Institute, The Johns Hopkins University Medical Institutions, Baltimore, MD); and the p53-inactive 2800T human fibroblasts, were kindly provided by Dr. Razmik Mirzayans

(Cross Cancer Institute, Edmonton, Canada). All cells were grown in DMEM/Ham's F12 medium with 10% FCS at 37°C and 5% CO_2.

Gel microdrop production

Cells in GMDs were prepared for each assay using a microdrop-maker (One Cell Systems, Cambridge, MA) as described in Bogen et al. (18). Briefly, cells were trypsinized, centrifuged and resuspended in phosphate buffered saline (PBS) with 0.5% FCS at 0.6 –1.0 x 10^6 cells/100 µl. After filtering the cells through a 20-µm nylon mesh (Small Parts, Miami Lakes, FL), 100 µl were added to 0.5 ml CelGel Encapsulation Matrix (One Cell Systems) together with 100 µl FCS and 10 µl Pluronic F68 (Sigma). This suspension was added to 15 ml CelMix Emulsion Matrix (One Cell Systems) and then emulsified using the GMD maker (1200 rpm at RT for 1 min; 1 min at 1200 rpm at 4°C; then at 600 rpm at 4°C for 8 min). Resulting GMDs were washed 3 times with HBSS, filtered through a 74-µm mesh and resuspended in culture media and either incubated or irradiated and incubated.

Radiation exposures

We used two different radiation dose rates for these experiments to give doses from 0 – 200 cGy. Encapsulated cells were irradiated at 0.18 cGy/min using a ^{137}Cs source (Picker International, Cleveland, OH) while being incubated at 37°C with 5% CO_2, or at 22 cGy/min in a J. L. Shepherd Mark I ^{137}Cs irradiator (San Fernando, CA) for relatively short times under ambient conditions.

Gel microdrop/flow cytometry (GMD/FC) assay of colony formation

At 96 h post-encapsulation, exposed and control GMDs were washed and resuspended in PBS and LIVE/DEAD® (LD) stain (2.5 μM ethidium homodimer, 75 nM calcein AM, Molecular Probes, Eugene OR). In each GMD/FC assay, 10^4 cell-bearing GMDs were analyzed by FACSort FC using Cellquest Software (Becton Dickinson, San Jose, CA). Linear forward-scatter (FSC) *vs* log scale side-scatter (SSC) plots were obtained as well as FL1 (log) *vs.* FL2 (log) plots (calcein AM *vs.* ethidium homodimer, respectively) for LD-stained GMDs. Dot-plot regions defining GMDs containing single (S) *vs.* multiple (M) cells were assigned based on corresponding S:M ratios estimated by microscopic analysis of control and treated GMDs at 96 h post-encapsulation. GMDs with single or multiple cells inside can be distinguished on an FSC-SSC dot-plot because they define different GMD populations based on the amount of scatter caused by the varying number of cells constituting the microdrop. From each GMD/FC analysis, the estimated fraction, $F_M = [M/(S+M)]$, of occupied GMDs that each contain a live microcolony was normalized to reflect a corresponding fraction relative to untreated F_M measured using unexposed concurrent control GMDs. Typically F_M of unirradiated controls was 85-90% after 4 days in culture.

Conventional colony-forming assay

Tumour cells were plated at 100 cells per 60-mm tissue culture dish, irradiated 4 h post-seeding and incubated for 8-10 days. Fibroblasts were plated at 300 cells per 100-mm culture dish and irradiated after 18 h of incubation. For colony forming assays requiring pifithrin, cells were incubated with 30 μM pifithrin for 16-20 h prior to irradiation and incubated a further 24 h in the presence of the drug. After 2-3 weeks, surviving cells forming visible colonies (containing > 50 cells) were counted after staining with crystal violet in 60% methanol.

Data analysis

Analysis of growth data plotted in Figure 1 was performed using constrained least-squares linear regression, and associated F-tests for fit; all these calculations were done using *Mathematica*® 4.2 software (Wolfram, Champaign, IL) (21, 22). To facilitate these analyses, regressions were performed using untransformed (rather than log-transformed) Y-axis (fractional) data values, in view of the fact that log-transformation is very nearly linear in the range of the Y-axis data obtained. Means and standard errors of the mean (S.E.M.) were calculated with reference to untreated controls to analyze data shown in Figs. 2-10. To test statistical significance of response differences, we performed 2-tail t-tests or analysis of variance (ANOVA) after in each case confirming variance homogeneity by F-test, using the Prism v. 3.03 graphics and statistics software package (GraphPad, San Diego, CA). Results were considered significant if $p \leq 0.05$.

Cell cycle analysis

Cell cycle analysis was performed on A549 cells after exposure to 0, 5, 10 and 20 cGy. Cells were seeded at 0.5×10^6 cells/dish, grown overnight, irradiated and then harvested at appropriate times up to 24 h. This consisted of trypsinization, fixation in 95% ethanol and treatment with 10 μg/ml RNase and 5 μg/ml propidium iodide (PI). Flow cytometry was used to analyze the resulting stained DNA and relative numbers of cells in each phase of the cell cycle were ascertained by ModFit software (Verity Software House, Topsham, MI).

Preparation of cell lysates

Cells were trypsinized and washed in PBS at 4°C. The pellet was resuspended in a modified RIPA buffer (150 mM NaCl; 50 mM Tris-HCl, pH 7.4; 1% NP-40, 0.25% sodium deoxycholate; 1 mM EGTA; 1 mM sodium orthovanadate; 1 mM sodium fluoride; 1 mM PMSF and protease inhibitor cocktail diluted 1:100). Cells were sheared with a 22-gauge needle, incubated on ice for 30 min and centrifuged at 13000 x *g* for 20 min at 4°C. The supernatant lysate was decanted into fresh tubes and stored frozen at -80°C.

Western blots

Immunoblotting was performed on lysates of A549 cells that had been irradiated at 0, 5, 10 and 20 cGy and either harvested immediately or incubated for appropriate times. After blocking with PBS-Tween 20 with 5% nonfat milk, the nitrocellulose blots were probed with various monoclonal and polyclonal antibodies and after washing, reactions were visualized by enhanced chemiluminescent detection of horseradish peroxidase (HRP)-conjugated secondary antibodies. Bands on the autoradiographs were quantified with a digitized image analyzer (23).

Apoptosis assays

Caspase-3: Cells were seeded in 60-mm culture dishes and grown overnight, then irradiated at 0 to 100 cGy at 22 cGy/min. Active caspase-3 levels were determined using an antibody kit developed by BD Biosciences. Briefly, cells are washed, fixed and permeabilized, then incubated with a FITC-conjugated caspase-3 antibody for 30 min. Relative amounts of active caspase-3 were quantified by flow cytometry following the protocol of Belloc et al. (24).

Annexin-V: Cells were seeded in 60-mm culture dishes and grown overnight, then irradiated at 0 to 100 cGy at 22 cGy/min. Trypsinized and washed cells were treated with propidium iodide (PI) and annexin V-FITC which binds to phosphatidylserine translocated to the exterior of the cell membrane early in the apoptosis pathway as well as during necrosis. Determinations were made 4 h after radiation doses to A549 and MCF7 cells and 6 h post irradiation of T98G, 2800T, GM38 and CRL2522 cells. The assay was performed as outlined in the Annexin-V-FITC kit protocol of the manufacturer (BD Biosciences) and cells were counterstained with propidium iodide to distinguish apoptosis from necrosis. Flow cytometry was employed to visualize the bound FITC, and necrotic cells (which were stained with both PI and FITC) were gated out so that an accurate determination of the percentage of apoptotic cells could be made (25).

Inhibition of p53 with pifithrin: Cells were treated with 3 μM or 30 μM pifithrin (PFT) for 2 h prior to irradiation, and the annexin-V assay was performed as described above.

Cell cycle status of annexin-V-FITC binding cells: A549 cells were treated as above for the annexin-V binding assay and then fixed in -20ºC 75% ethanol for 30 min at -20ºC. The fixed cells were washed twice with PBS and then stained with 5 μM PI in PBS with 2 μg/ml RNase for 30 min in preparation for flow cytometry. During FC we gated on the fraction of cells that had bound annexin-V-FITC and determined their cell cycle status (by examining their content of DNA stained with PI), comparing them to the cell cycle status of cells in the total cell population.

Results

Cell Proliferation: We employed the GMD/FC approach to follow early growth of single A549, T98G and MCF7 cells into GMD encapsulated microcolonies. Optimum detection of altered relative proliferative capacity of singly encapsulated cells was determined to be ~4 days post GMD-encapsulation both with and without irradiation at 22 or 0.18 cGy/min (data not shown). The analysis of A549 and T98G cells irradiated at 22 cGy/min yielded clear evidence of HRS (Fig. 1). MCF7 cells, on the other hand, did not exhibit this hypersensitivity (Fig. 1). Similar HRS/IRR responses were also apparent in the A549 and T98G cells when irradiated at 0.18 cGy/min (Fig. 1). To confirm the data obtained with the GMD/FC assay, we carried out conventional clonogenic survival assays with all three cell lines. The survival curves (Fig. 2) matched the GMD/FC data showing an HRS response for A549 and T98G cells but not for MCF7 cells.

Cell Cycle Analysis: To begin to identify possible mechanisms for the hypersensitivity exhibited in the GMD/FC assay, we examined the relative numbers of A549 cells in various phases of the cell cycle at times up to 24 h after irradiation at 5, 10 and 20 cGy in comparison to unirradiated cells (Fig. 3). We were specifically interested in differences between 10 cGy-irradiated cells, a dose at which A549 cells display HRS, and 5 and 20 cGy. After irradiation at 22 cGy/min no statistically significant differences were observed between the three doses in any phase of the cell cycle. A small, but statistically significant, difference was observed for cells in G_2/M after 10 cGy irradiation at 0.18 cGy/min; i.e. more cells appeared in G_2/M at 6 and 12 h post irradiation. However, since this result was not observed with the higher dose rate, it is unlikely to be specifically related to HRS.

In addition to flow cytometric cell cycle analysis, we also examined cyclin B1 (p62) and cdk1 (p34) protein levels in irradiated A549 cells (0.18 cGy/min) to ascertain whether they were affected at these low doses. Badie et al. (26) have shown that both cdk1 and cyclin B1 protein levels are down regulated in response to DNA damage in cells with functional p53 at higher radiation doses. Figure 4 shows accumulated data from densitometry performed on five immunoblots all corrected for protein concentration relative to actin (p43). The results indicate that both proteins are down-regulated at these low doses relative to controls, but the differences seen between 5, 10 and 20 cGy were not statistically significant ($p>0.05$).

Apoptotic responses: We chose to examine two independent parameters of initiation of apoptosis following irradiation of A549, T98G and MCF7 cells: caspase-3 activation and phosphatidylserine translocation. During apoptosis caspase-3 is cleaved into its active form, a heterodimer of 17 and 12 kDa subunits, which can proteolytically cleave other cellular enzymes, including poly(ADP-ribose) polymerase (27). As a marker of apoptosis, caspase-3 activation is typically measured 24 h and later after the cellular damage. Figure 5 shows the dose responses we obtained with a flow cytometric assay for active caspase-3. A549 and T98G cells showed a discernable activation of caspase-3 at the doses that induce HRS. MCF7 cells, which displayed no significant caspase-3 activation in agreement with Jaenicke et al. (20), served as a negative control.

A second marker of apoptosis is the translocation of phosphatidylserine to the exterior of the cell membrane, which can be detected by binding of fluorescently tagged annexin-V (25). Transfer of phosphatidylserine is considered an early to intermediate event in the apoptotic process (28), and

consequently, the annexin-V assay has been applied at times after cellular insult ranging from 2-24 h. We therefore examined annexin-V binding to A549 cells after irradiation at 0, 5, 15 and 25 cGy for times up to 24 h. The response (Fig. 6a and b) indicated optimum binding at 4 h. Similarly, we observed optimum binding to T98G cells at 6 h after irradiation (data not shown). No significant annexin-V binding was seen with MCF7 cells at any time up to 24 h. A more complete dose response at 4 h (A549 and MCF7) and 6 h (T98G) is shown in Figure 6c. In the same assay the cells were also stained with PI, which is used to gauge cell permeability as a measure of necrosis. The irradiated cells (A549, T98G and MCF7) showed no significant increase in uptake of PI in comparison to unirradiated cells at the doses at which HRS was observed (data not shown). We also examined the cell cycle status of the A549 cells binding annexin-V 4 h after 10 cGy irradiation (~ 4% of the total irradiated cell population) in comparison to the cell cycle status of cells in the total irradiated population (Fig. 6d). The data indicate that the cell cycle distribution of irradiated cells that bound annexin-V was fairly similar to the distribution of the total irradiated cell population. The most significant difference between the two populations was the proportionally low level of G_2/M cells binding annexin-V (6% *vs.* 12%), and a concomitant increase in the percentage of cells in G_1 binding annexin-V (43% *vs.* 38%).

Role of p53 in the HRS apoptotic response: The tumour suppressor, p53, is considered a key regulator of the apoptotic pathway (29). All three tumour cell lines used in this study express p53, although p53 in T98G cells is mutated at Met-237. We therefore examined the potential participation of p53 in the initiation of the apoptotic response by irradiation of the cells in the presence of pifithrin, an inhibitor of p53-mediated apoptosis (30), and then measuring annexin-V

binding 4 h (A549 and MCF7) and 6 h (T98G) after irradiation. The data (Fig. 7) show that 3-μM pifithrin eliminated the annexin-V-FITC signal previously observed at the HRS doses with A549 and T98G cells. We followed up this experiment by testing the influence of pifithrin on HRS itself. Figure 8 reveals that treating A549 and T98G cells with pifithrin completely ablated HRS. Finally, we compared the low-dose hypersensitivity of HCT116 $p53^{+/+}$ cells and $p53^{-/-}$ cells generated by targeted disruption of the p53 alleles in HCT116 cells (31). The survival curves (Fig. 9) confirm the association of active p53 with HRS.

HRS in human fibroblasts: Because tumour cell lines by their nature often possess more than one mutation that may affect apoptotic pathways, we sought to further confirm our results in non-cancerous and non-transformed human cells. To date, such cells have not been extensively examined for HRS; the only report being that of a study of L132 human epithelial cells (32). Consequently we analyzed the HRS and apoptotic responses of three human fibroblast strains, CRL2522, GM38 and 2800T. The first two possess wild type p53 activity, while 2800T cells lack active p53 (33). The results, shown in Figure 10, indicate that the two normal cell lines displayed a typical HRS response as well as annexin-V binding and elevated caspase-3, but the 2800T cells showed no indication of HRS or apoptosis.

Discussion

The GMD/FC assay was found to be an efficient method to follow initial proliferation of single A549, T98G and MCF7 cells into GMD encapsulated microcolonies, the evolution of which could be followed with or without prior exposure to radiation. The advantage of this technique, as with other flow cytometry-based assays, is the capacity to analyze a relatively large number of

individual cells, or in this case, gel microdrops (we were unable to apply this approach to normal human fibroblasts because of a tendency for these cells to escape the microdrops.)

In A549 cells exposed to 0 to 100 cGy at 22 cGy/min, the GMD/FC data indicate a nonlinear, non-monotonic dose-survival response at the lower doses; i.e., there was significant hypersensitivity at 10 to 17.5 cGy. If combined data for the 10, 15 and 17.5 cGy exposure groups are excluded, goodness-of-fit analysis indicates that all other data points obtained are consistent with a linear-quadratic fit ($p = 0.28$, i.e. no significant departure from the pattern predicted by a linear-quadratic fit), whereas that fit is rejected if the 10 to 17.5 cGy data are included ($p \approx 0$) (Fig. 1). Similar results were also obtained for T98G cells in GMDs, but no radiation hypersensitivity was observed in similarly exposed MCF7 cells (Fig. 1). These findings are consistent with recent evidence of low dose hypersensitivity in many tumor cell lines (but not in MCF7 cells) exposed chronically to low dose low LET radiation reported by Joiner et al. (8) and by Michael Joiner (personal communication), who have applied automated imaging techniques to increase the ability of the classical colony forming assay to detect small reductions in clonogenic survival at low level irradiation. The GMD/FC data, as well as the apoptosis results, demonstrate that hypersensitivity in A549 and T98G cell lines occurs during the first cell cycle after low dose irradiation, and argue against the possibility that HRS is the result of a longer-term consequence, such as accrual of chromosome damage in descendents of the irradiated cells seen after high dose irradiation (34).

In addition to examining cell proliferation at 22 cGy/min, we also looked at the response to radiation delivered at a 100-fold lower dose rate (0.18 cGy/min). This dose rate is equivalent to

~10 cGy/h, which is the dose rate estimated by Fowler (35) to be the maximum dose intensity to tumor cells that can be achieved with radioimmunotherapy (RIA). As mentioned in the introduction, a lower dose rate would be expected to be more effective at inducing HRS if a phase of the cell cycle was associated with HRS, because more cells would have the opportunity to move through this phase of the cell cycle during irradiation (6). This approach to analyzing HRS dependence on cell cycle status proved inconclusive because neither the A549 nor the T98G cells showed such an enhancement of HRS at the lower dose rate (Fig. 1).

Our examination of the effects of low doses of radiation on cell cycle checkpoints (Figs. 3 and 4), including expression of key proteins, failed to reveal any indication that the doses inducing maximal HRS had a different effect on the cell cycle than the other doses below 50 cGy. This is in general agreement with others (14, 36), although Hendrikse et al. (37) reported a modest arrest in G_2/M, but no change in cyclin B1, after irradiation of a lymphoblast cell line (TK6) with 10 and 30 cGy.

To date there has been no clear identification of the mode of death - necrosis, apoptosis or senescence - of the cells dying at low dose. Part of the problem has been identifying the fate of a small component of the cell population. We chose to use two well-characterized and independent markers of apoptosis, caspase-3 activation and annexin-V binding to translocated phosphatidylserine, because both could be monitored by flow cytometry, a technique that measures cell characteristics on a cell by cell basis. Our data indicate that apoptosis plays a role in the death of A549 and T98G cells after low dose radiation (Figs. 5 and 6). Although the percentage of apoptotic cells identified by FC was small, the data were consistent over the many

times that each assay was repeated. Further credence can be given to the data because (a) neither assay identified an increase in apoptotic MCF7 cells, in line with its lack of HRS response noted above, and (b) the apoptotic response seen with A549 and T98G cells closely correlated with the dose response seen for HRS. We are aware that others have used a similar approach to look for apoptosis in cells displaying HRS without success (14). We are not sure why these assays failed to reveal apoptosis, but one possibility may lie in the timing of the assays after irradiation. For example, we observed that the difference in annexin-V binding between irradiated A549 cells and control cells reached a maximum at 4 h and was negligible by 24 h (Fig. 6b), the latter unfortunately being the time at which others (14) looked for binding.

The tumor suppressor protein p53 has been shown to be involved in ionizing radiation-induced caspase-3 activation and apoptosis at 4 Gy (38). In order to examine whether p53 played a role in the low-dose apoptosis, we employed a p53 inhibitor, pifithrin, which was originally identified by screening a chemical library for inhibitors of p53 transactivation and then for suppression of p53-dependent apoptosis (30). A549 cells express wild type active p53 (39) and T98G cells express p53 with a point mutation in codon 237 (40). While this point mutation severely reduces the transactivation of several genes, including CDKN1A ($p21^{WAF1,\ Cip1}$), it does not appear to suppress p53-dependent apoptosis in response to agents such as camptothecin (41). The loss of annexin-V binding to cells irradiated in the presence of pifithrin (Fig. 7) provided evidence for p53 involvement in the low-dose apoptosis. This was confirmed by showing firstly that pifithrin ablated HRS in A549 and T98G cells (Fig.8), and secondly that p53-inactive human cell lines did not display HRS while p53 wild-type controls had normal HRS responses (Figs. 9 and 10).

We have provided evidence that low dose irradiation of A549 and T98G cells giving rise to HRS does not lead to readily discernable cell cycle arrest, but does induce p53-dependent apoptosis. When we compared the cell cycle status of the subpopulation of A549 cells binding annexin-V to the total 10-cGy irradiated cell population (Fig. 6d), we observed that the overall difference between the two populations was not substantial and was primarily confined to a decreased proportion of cells in G_2/M binding annexin-V and a concomitant increase in annexin-V binding cells in G_1. These measurements were taken 4 h after irradiation. Since this time is too short for the cells to traverse more than one phase of the cell cycle (e.g. from G_2/M to S), this would suggest that the apoptosis responsible for HRS can be triggered by irradiation in any phase of the cell cycle. At first sight this would appear to contradict the observation by Short et al. (12) of a more pronounced HRS/IRR response in cell populations enriched for G_2 at the time of irradiation in comparison to populations enriched for G_1 or S phase. However, both sets of observations can be reconciled if the ATM-dependent early G_2 checkpoint (13), proposed by Marples and Joiner (9, 10) to mediate the switch from HRS to IRR, regulates p53-dependent apoptosis. If cells pass through this checkpoint relatively soon after irradiation and if their DNA damage is repairable, the checkpoint would serve to prevent the apoptosis. On the other hand, cells reaching the checkpoint at later times would be further along the apoptotic pathway and less responsive to stop signals. Thus a population of cells enriched for G_2 when irradiated would have to traverse the complete cell cycle before encountering the checkpoint and, therefore, undergo higher levels of apoptosis than a population enriched for G_1 or S. This explanation would also account for the comparatively low level of G_2 cells binding annexin-V seen in Figure 6d because a high percentage of these cells would have been in S phase 4 h earlier when the cells were irradiated.

The dose relationship between HRS and IRR would thus reflect a combination of (a) a stochastic process giving rise to a percentage of cells that receive sufficient damage to elicit p53-dependent apoptosis before passing through the early G_2 checkpoint, and (b) a potential dose-dependent activation of the checkpoint. In their description of the early G_2 checkpoint found in HeLa cells, Xu et al. (13) noted a diminution in the activity of the checkpoint at doses <40 cGy, and thereafter activity appears to be dose independent. Such a 'threshold' dose would probably vary from cell line to cell line, which may explain, at least in part, the variation in HRS/IRR responses seen among different cell lines.

Acknowledgements

This work was performed in part under the auspices of the U.S. Department of Energy by the University of California, Lawrence Livermore National Laboratory under contract No. W-7405-Eng-48, and was supported by grants from the National Cancer Institute of Canada, the Alberta Cancer Board, and the U.S. DOE Low Dose Radiation Research Program. We thank Dr. Brian Marples (Wayne State University) and Dr. David Murray (Cross Cancer Institute) for their helpful discussion.

References

1. Upton, A. C. Carcinogenic effects of low-level ionizing radiation: problems and prospects. In Vivo 16:527-533, 2002.
2. Murtha, A. D. Review of low-dose-rate radiobiology for clinicians. Seminars in Radiat. Oncol. 10:133-138, 2000.
3. Marples, B., and Joiner, M. C. The response of Chinese hamster V79 cells to low radiation doses: Evidence of enhanced sensitivity of the whole cell population. Radiat. Res. 153:41-51, 1993.
4. Joiner, M. C., Lambin, P., Malaise, E. P., Robson, T., Arrand, J. E., Skov, L. A., and Marples, B. Hypersensitivity to very-low single radiation doses: Its relationship to the adaptive response and induced radioresistance. Mutat. Res. 358:171-183, 1996.
5. Wouters, B. G., and Skarsgard, L. D. The response of a human tumor cell line to low radiation doses: evidence of enhanced sensitivity. Radiat. Res. 138:S76-80, 1994
6. Wouters, B. G., Sy, A. M., and Skarsgard, L. D. Low-dose hypersensitivity and increased radioresistance in a panel of human tumor cell lines with different sensitivity. Radiat. Res. 146:399-413, 1996.
7. Wouters, B. G., and Skarsgard, L. D. Low-dose radiation sensitivity and induced radioresistance to cell killing in HT-29 cells is distinct from the "adaptive response" and cannot be explained by a subpopulation of sensitive cells. Radiat. Res. 148:435-442, 1997.
8. Joiner, M. C., Marples, B., Lambin, P., Short, S. C., and Turesson, I. Low-dose hypersensitivity: current status and possible mechanisms. Int. J. Radiat. Oncol. Biol. Phys. 49:379-389, 2001.

9. Marples, B., Wouters, B. G., Collis, S. J., Chalmers, A. J., and Joiner, M. C. Low-dose hyper-radiosensitivity: a consequence of ineffective cell cycle arrest of radiation-damaged G2-phase cells. Radiat. Res. 161:247-1255, 2004.
10. Marples, B. Is low-dose hyper-radiosensitivity a measure of G2-phase cell radiosensitivity? Cancer Metastasis Rev. 23:197-207, 2004.
11. Marples, B., and Joiner, M. C. Modification of survival by DNA repair modifiers: a probable explanation for the phenomenon of increased radioresistance. Int. J. Radiat. Biol. 76:305-312, 2000.
12. Short, S. C., Woodcock, M., Marples, B., and Joiner, M. C. Effects of cell cycle phase on low-dose hyper-radiosensitivity. Int. J. Radiat. Biol. 79:99-105, 2003.
13. Xu, B., Kim, S. T., Lim, D. S., and Kastan, M. B. Two molecularly distinct G(2)/M checkpoints are induced by ionizing irradiation. Mol. Cell. Biol. 22:1049-1059, 2002.
14. Chandra, S., Dwarakanath, B. S., Khaitan, D., Mathew, T. L., and Jain, V. Low-dose radiation hypersensitivity in human tumor cell lines: Effects of cell-cell contact and nutritional deprivation. Radiat. Res. 157:516-525, 2002.
15. Short, S. C., Mitchell, S. A., Boulton, P., Woodcock, M., and Joiner, M. C. The response of human glioma cell lines to low-dose radiation exposure. Int. J. Radiat. Biol. 75:1341-1348, 1999.
16. Weaver, J. C., Bliss, J. G., Harrison, G. I., Powell, K. T., and Williams, G. B. Microdrop technology: A general method for separating cells by function and composition. Methods: A Companion to Methods in Enzymology 2: 234-247, 1991.
17. Goguen, B., and Kedersha, N. Clonogenic cytotoxicity testing by microdrop encapsulation. Nature 363:189-190, 1993.

18. Bogen, K. T., Enns, L., Hall, L. C., Keating, G. A., Weinfeld, M., Murphy, G., Wu, R. W., and Pantelakos, F. N. Gel microdrop flow cytometry assay for low-dose studies of chemical and radiation cytotoxicity. Toxicology 160:5-10, 2001.

19. Short, S., Mayes, C., Woodcock, M., Johns, H., and Joiner, M. C. Low dose hypersensitivity in the T98G human glioblastoma cell line. Int. J. Radiat. Biol. 75:847-855, 1999.

20. Jaenicke, R. U., Sprengart, M. L., Wati, M. R. and Porter, A. G. Caspase-3 is required for DNA fragmentation and morphological changes associated with apoptosis. J. Biol. Chem. 273:9357-9360, 1998.

21. Selvin, S. *Practical Biostatistical Methods*. Duxbury Press, Wadsworth Publishing Co., Belmont, CA. 1995.

22. Wolfram S. *The Mathematica Book*. 4th ed. Cambridge University Press, Cambridge, UK. 1999.

23. Palcic, B. and Jaggi, B. *Bioinstrumentation: Research, Developments and Applications*. Wise, D. L. (ed.) Butterworth Stoneham, MA. pp 923-991, 1990.

24. Belloc, F., Belaud-Rotureau, M. A., Lavignolle, V., Bascans, E., Braz-Pereira, E., Durrieu, F., and Lacombe, F. Flow cytometry detection of caspase-3 activation in preapoptotic leukemic cells. Cytometry 40:151-160, 2000.

25. van Engeland, M., Ramekers, F. C. S., Schutte, B., and Reutelingsperger, C. P. M. A novel assay to measure loss of plasma membrane asymmetry during apoptosis of adherent cells in culture. Cytometry 24:131-139, 1996.

26. Badie, C., Itzhaki, J. E., Sullivan, M. J., Carpenter, A. J., and Porter, A. C. Repression of CDK1 and other genes with CDE and CHR promoter elements during DNA damage-induced G_2/M arrest in human cells. Mol. Cell. Biol. 20:2358-2366, 2000.

27. Patel, T., Gores, G. J., and Kaufmann, S. H. The role of proteases during apoptosis. FASEB J. 10:587-597, 1996.

28. Smyth, P. G., Berman, S. A., and Bursztajn, S. Markers of Apoptosis: Methods for elucidating the mechanism of apoptotic cell death from the nervous system. BioTechniques 32:648-665, 2002.

29. Levine, A. J. p53, the cellular gatekeeper for growth and division. Cell 88:323-331, 1997.

30. Komarov, P. G., Komorova, E. A., Kondratov, R. V., Christov-Tselkov, K., Coon, J. S., Chernov, M. V., and Gudkov, A. V. A chemical inhibitor of p53 that protects mice from the side effects of cancer therapy. Science 285:1733-1737, 1999.

31. Bunz, F., Dutriaux, A., Lengauer, C., Waldman, T., Zhou, S., Brown, J. P., Sedivy, J. M., Kinzler, K. W., and Vogelstein, B. Requirement for p53 and p21 to sustain G2 arrest after DNA damage. Science 282:1497-1501, 1998.

32. Singh, B., Arrand, J. E., and Joiner, M. C. Hypersensitive response of normal human lung epithelial cells at low radiation doses. Int. J. Radiat. Biol. 65:457-464, 1994.

33. Barley, R. D. C., Enns, L., Paterson, M. C. and Mirzayans, R. Aberrant p21(WAF1)-dependent growth arrest as the possible mechanism of abnormal resistance to ultraviolet light cytotoxicity in Li-Fraumeni syndrome fibroblast strains heterozygous for TP53 mutations. Oncogene 17:533-541, 1998.

34. Mothersill, C., Kadhim, M. A., O'Reilly, S., Papworth, D., Marsden, S. J., Seymour, C. B., and Wright, E. G. Dose- and time-response relationships for lethal mutations and chromosomal instability induced by ionizing radiation in an immortalized human keratinocyte cell line. Int. J. Radiat. Biol. 76:799-806, 2000.

35. Fowler, J. F. Radiobiological aspects of low dose rates in radioimmunotherapy. Int. J. Radiat. Oncol. Biol. Phys. 18:1261-1269, 1990.

36. Mitchell, C. R., Folkard, M., and Joiner, M. C. Effects of exposure to low-dose-rate ^{60}Co gamma rays on human tumor cells in vitro. Radiat. Res. 158:311-318, 2002.

37. Hendrikse, A. S., Hunter, A. J., Keraan, M., and Blekkenhorst, G. H. Effects of low dose irradiation on TK6 and U937 cells: induction of p53 and its role in cell-cycle delay and the adaptive response. Int. J. Radiat. Biol. 76:11-21, 2000.

38. Yu, Y., and Little, J. B. p53 is involved in but not required for ionizing radiation-induced caspase-3 activation and apoptosis in human lymphoblast cell lines. Cancer Res. 58:4277-4281, 1998.

39. Lu, W., Lin, J., and Chen, J. Expression of p14ARF overcomes tumor resistance to p53. Cancer Res. 62:1305-1310, 2002.

40. Ullrich, S. J., Sakaguchi,K., Lees-Miller, S. P., Fiscella, M., Mercer, W. E., Anderson, C. W., and Appella, E. Phosphorylation at Ser-15 and Ser-392 in mutant p53 molecules from human tumors is altered compared to wild-type p53. Proc. Natl. Acad. Sci. USA 90:5954-5958, 1993.

41. Weller, M., Winter, S., Schmidt, C., Esser, P., Fontana, A., Dichgans, J., and Groscurth, P. Topoisomerase-I inhibitors for human malignant glioma: Differential modulation of p53, p21, bax and bcl-2 expression and of CD95-mediated apoptosis by camptothecin and β-lapachone. Int. J. Cancer 73:707-714, 1997.

42. Heyer, B. S., MacAuley, A., Behrendtsen, O., and Werb, Z. Hypersensitivity to DNA damage leads to increased apoptosis during early mouse development. Genes Dev. 14:2072-2084, 2000.

Figure legends

Figure 1. Cell proliferation determined by the GMD/FC assay for A549, T98G and MCF7 cells irradiated with doses up to 2 Gy delivered at 22 cGy/min or 0.18 cGy/min. Data points (and error bars) each represent the mean (± 1 S.E.M.) of *n* independent dose-specific determinations (each from 10^4 cells) of cell growth in exposed relative to unexposed GMDs, ~95% of which contained a single cell at the time of exposure (S.E.M. = standard error of the mean). Values of *n* (from lowest to highest dose) are as follows. For A549 cells *n* = {17, 11, 11, 14, 13, 11, 11, 10, 2} (22 cGy/min), and *n* = {111, 24, 22, 46, 19, 30, 42, 33, 33, 3} (0.18 cGy/min); for T98G cells *n* = {15, 9, 9, 10, 13, 13, 10, 11} (22 cGy/min), and *n* = {21, 12, 12, 12, 9, 12, 6, 13, 11} (0.18 cGy/min); for MCF7 cells *n* = {17, 14, 15, 15, 13, 10, 11} (22 cGy/min). Solid circles represent data points that are statistically inconsistent ($p < 10^{-7}$) with (constrained) linear-quadratic fits to all data in each plot; similar fits (dashed curves) are all statistically consistent ($p > 0.01$) with the remaining data (open circles) shown in each plot.

Figure 2. Comparison of the cell proliferation, as determined by the GMD/FC assay (solid symbols), to cell survival, as determined by the colony forming assay (open symbols), for A549 cells irradiated at 22 cGy/min, T98G cells irradiated at 0.18 cGy/min and MCF7 cells irradiated at 22 cGy/min. The data for the colony forming assays represent the means of at least 3 independent assays. Error bars are ± S.E.M.

Figure 3. Cell cycle analysis of A549 cells. The cells were irradiated at either 22 cGy/min (left panels) or 0.18 cGy/min (right panels) for times up to 24 h after irradiation with 5 cGy (■), 10

cGy (□) or 20 cGy (●). The points show the means of 3-7 (22 cGy/min) and 5-10 (0.18 cGy/min) determinations. The error bars show ± S.E.M. and the p values were calculated by ANOVA.

Figure 4. Analysis of cyclin B1 (p62) and cdk1 (p34) protein levels in A549 cells in response to irradiation at 0.18 cGy/min to doses of 0, 5, 10 and 20 cGy. The upper panel shows a representative western blot and the lower panel displays the data accumulated from densitometry performed on cyclin B1(p62) and cdk1(p34) bands relative to actin (p43) on 5 (cyclin B1) and 4 (cdk1) separate blots. There was no significant difference found between 5, 10 and 20 cGy for cyclin B1 ($p=0.57$) or cdk1 ($p=0.88$). The cdk1 untreated control was significantly different from the irradiated samples ($p=0.0096$). Error bars show ± S.E.M. and p values were calculated by t-test.

Figure 5. Activation of caspase-3 24 h after irradiation of A549 (■), T98G (○) and MCF7 cells (□) at a dose rate of 22 cGy/min. In A549 cells there was a significant difference ($p<0.005$) between the unirradiated control and each of the 10, 15 and 100 cGy dose responses (*). For T98G cells there was a significant difference between the control and the 10 and 20 cGy doses ($p<0.05$). For both A549 and T98G cells the 10 and 20 cGy dose responses are significantly different from the dose response of MCF7 cells ($p<0.0001$). The data points represent data accumulated from 7-10 independent repeats. Error bars show ± S.E.M. and p values were calculated by t-test or ANOVA as appropriate. See Materials and Methods for details of the assay.

Figure 6. Translocation of phosphatidylserine as determined by the annexin-V-FITC binding assay after irradiation at 22 cGy/min (see Materials and Methods for experimental details). **(a)** Representative FC plots of A549 cells stained 2, 4, 8 or 24 h after irradiation with 0, 15 or 25 cGy. Annexin-V quantitation is based on the percent of cells in the lower right quadrant. **(b)** Plot of the time course for annexin-V binding based on 5 independent assays. Significant differences (see below) are indicated on the bar chart. The p values were calculated by t-test. **(c)** Dose response for annexin-V-FITC binding to A549 cells (■), MCF7 cells (□) and T98G cells (○). A549 and MCF7 cells were examined 4 h after irradiation and T98G cells 6 h after irradiation. For the A549 dose response curve, $p=<0.002$ at 10 and 20 cGy when compared to the unirradiated control. Values at 50 and 100 cGy are also different from control ($p<0.02$). T98G cells had significantly more annexin-V bound after 10 and 20 cGy doses ($p<0.01$) than they did prior to irradiation. By ANOVA, radiation doses of 10 and 20 cGy to A549 and T98G cells caused significantly more annexin-V binding than in MCF7 cells ($p<0.005$). The data points are the means of the values obtained from 9-14 (A549), 5 (MCF7) and 7-11 (T98G) independent experiments ± S.E.M. and p values were calculated using a t-test. Significant differences are marked (*) on the graph. **(d)** Cell cycle status 4 h post irradiation (10 cGy) of the total population of A549 cells compared with the status of the subpopulation binding annexin V-FITC. Significant differences between total cells and annexin-V binding cells are marked on the plot. Error bars show ± S.E.M. and p values were calculated by t-test.

Figure 7. Influence of the p53 inhibitor, pifithrin at 3 μM (□), compared to no pifithrin (■) as determined by the annexin-V binding assay. Significant differences ($p < 0.05$) are marked (*).

Each point represents the mean ± S.E.M. of 3-4 independent determinations. Top panel – A549 cells, middle panel – T98G cells, bottom panel – MCF7 cells.

Figure 8. Effect of 30 μM PFT on A549 and T98G cells as measured by a low-dose radiation dose response colony forming assay. N is at least 3 separate experiments for each point. Error bars indicate ± S. E. M.

Figure 9. Survival of $p53^{+/+}$ and $p53^{-/-}$ HCT116 cells to low-dose radiation measured by colony forming assay. N is at least 3 separate experiments for each point. Error bars indicate ± S. E. M.

Figure 10. Responses of human fibroblasts to low-dose radiation: Top panel – colony-forming assay; middle panel – annexin-V-FITC binding; bottom panel – anti-active-caspase-3 binding. There were at least 3 determinations for each point. Error bars indicate ± S. E. M.

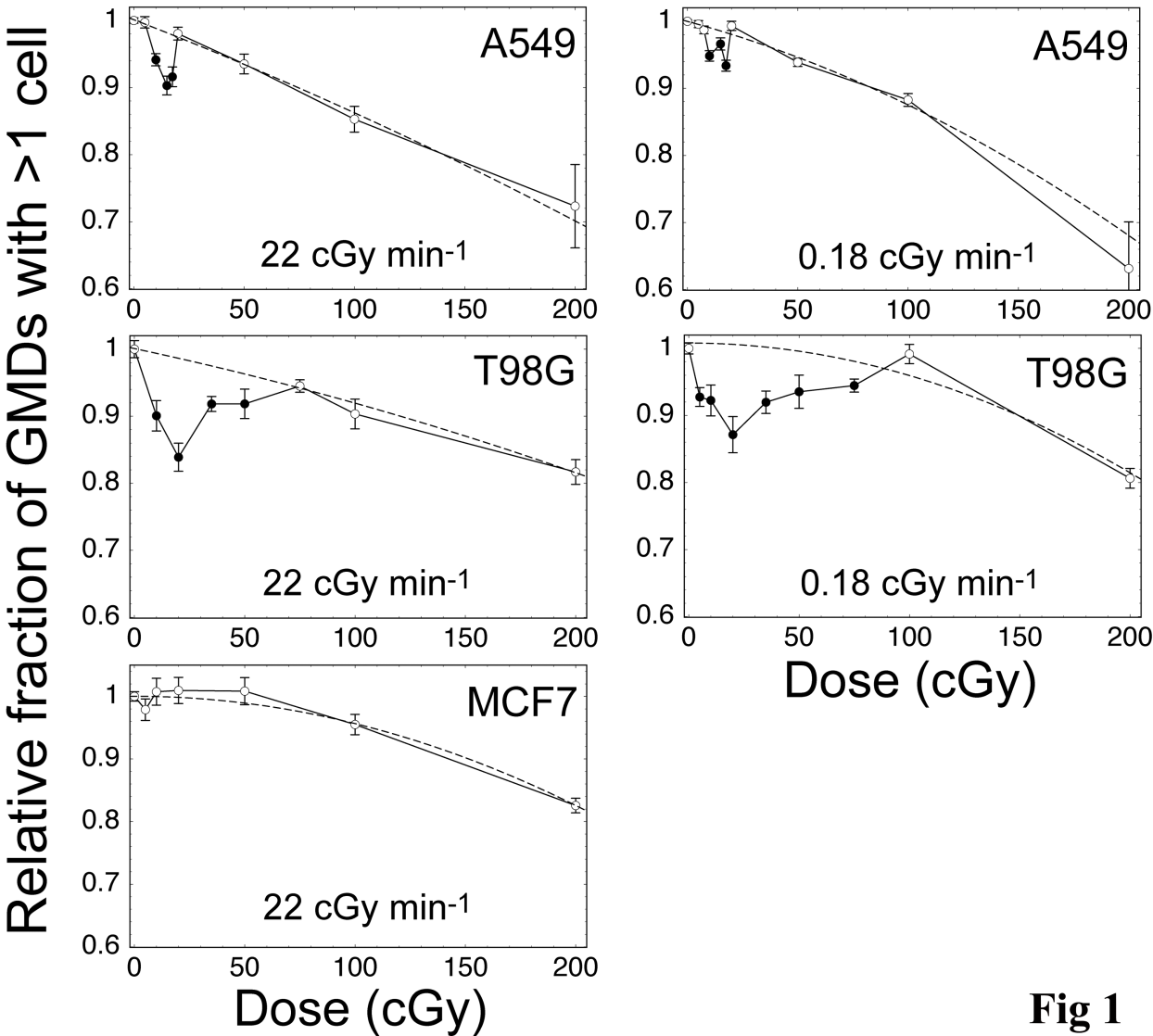
Relative fraction of GMDs with >1 cell
A549
22 cGy min-1
A549
0.18 cGy min-1
T98G
22 cGy min-1
T98G
0.18 cGy min-1
MCF7
22 cGy min-1
Dose (cGy)
Dose (cGy)
1
0.9
0.8
0.7
0.6
0
50
100
150
200

Fig 1

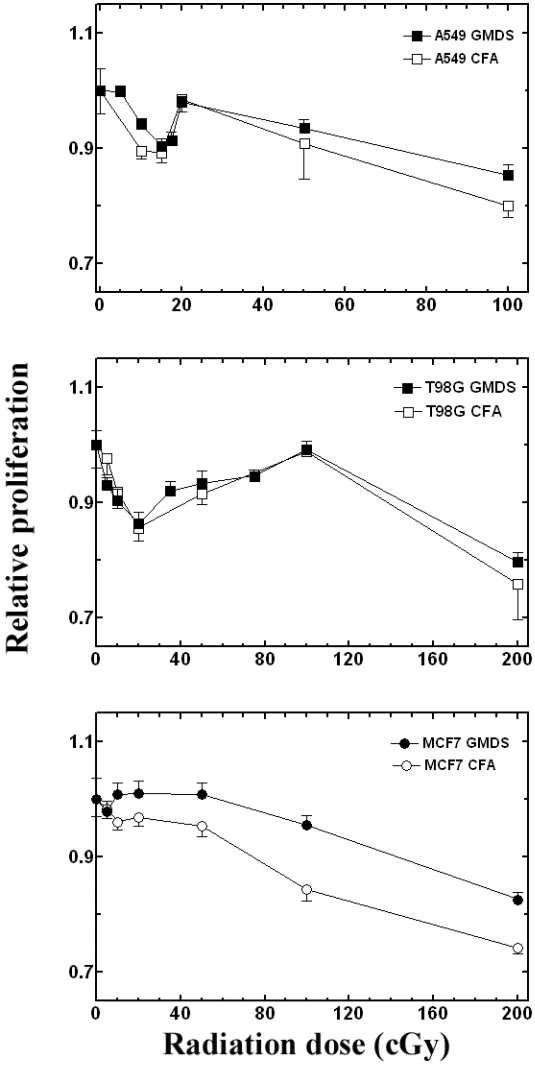
A549 GMDS
A549 CFA
T98G GMDS
T98G CFA
MCF7 GMDS
MCF7 CFA
Relative proliferation
Radiation dose (cGy)
1.1
0.9
0.7
0
20
40
60
80
100
120
160
200

Fig 2

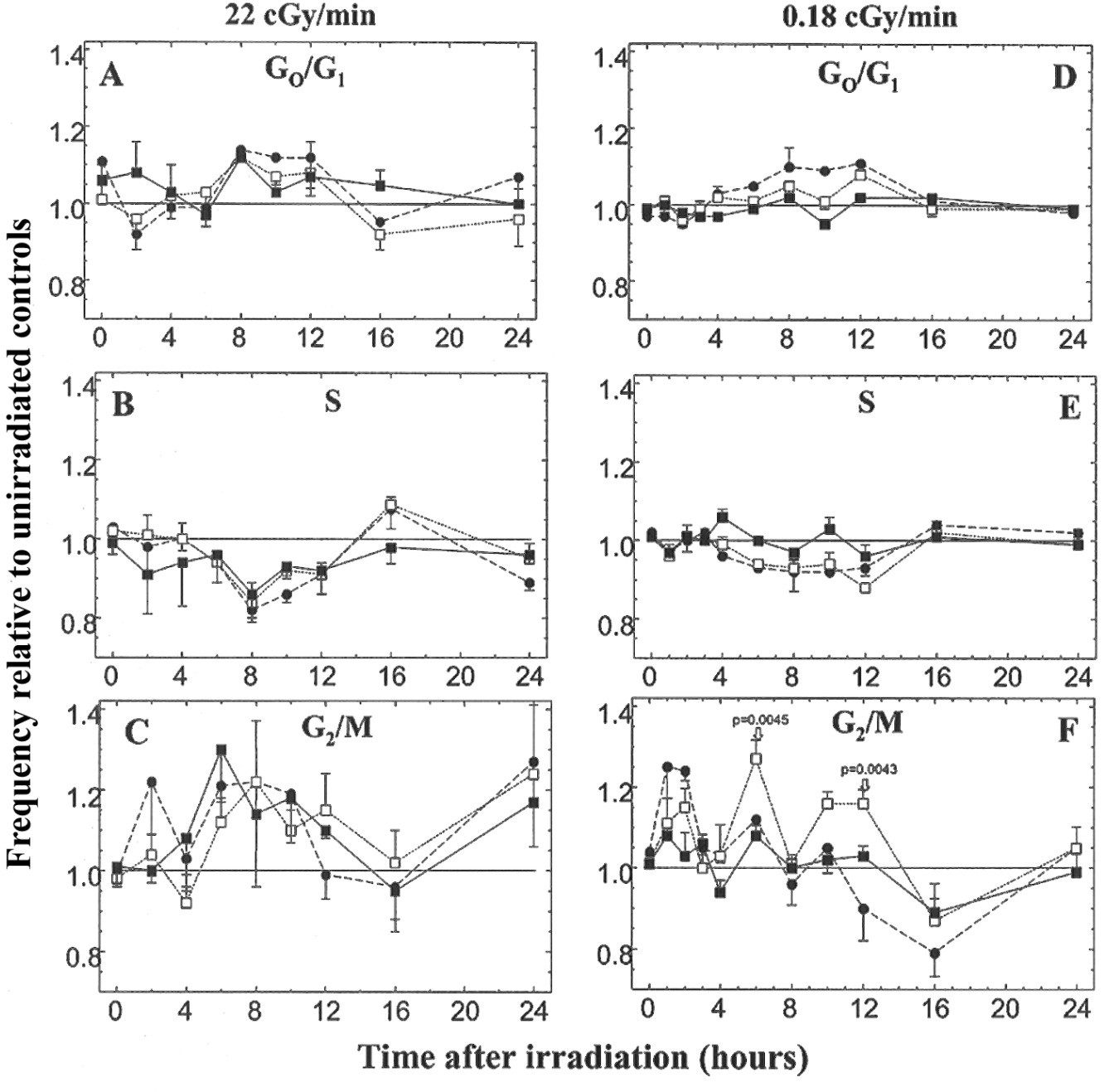
22 cGy/min
0.18 cGy/min
A
G_0/G_1
D
G_0/G_1
B
S
E
S
C
G_2/M
F
G_2/M
p=0.0045
p=0.0043
Frequency relative to unirradiated controls
Time after irradiation (hours)

Fig 3

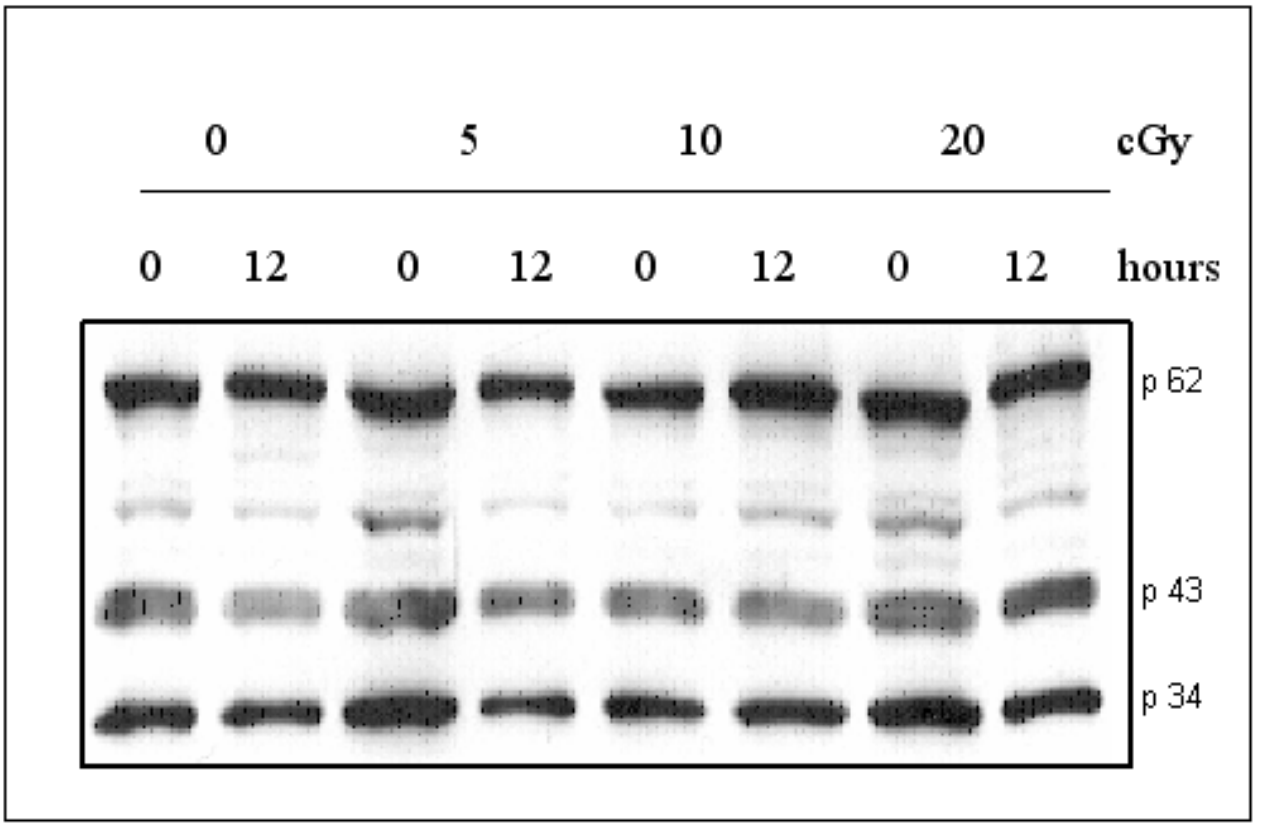
0
5
10
20
cGy
0
12
0
12
0
12
0
12
hours
p 62
p 43
p 34

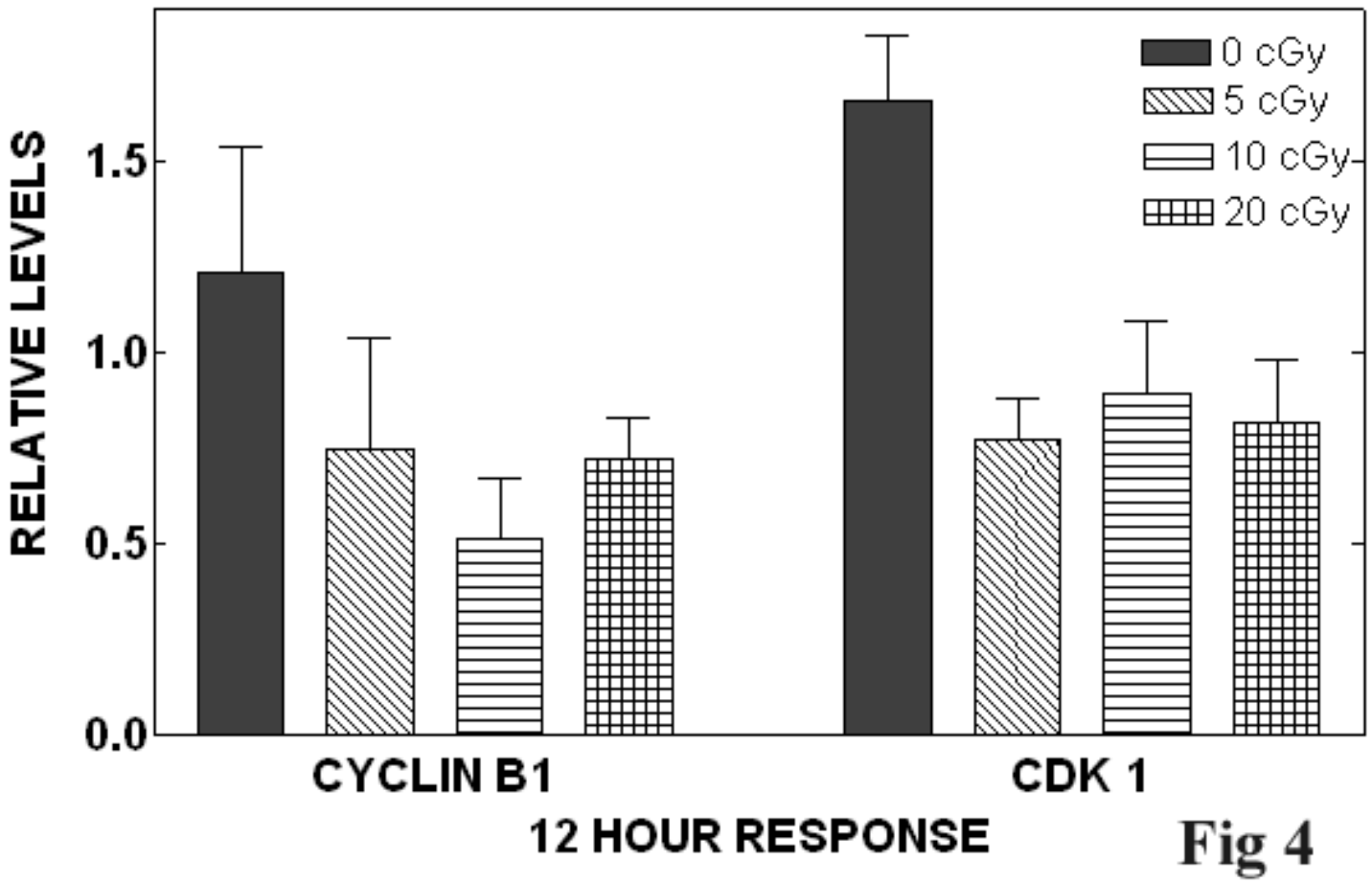
0 cGy
5 cGy
10 cGy
20 cGy
RELATIVE LEVELS
1.5
1.0
0.5
0.0
CYCLIN B1
CDK 1
12 HOUR RESPONSE

Fig 4

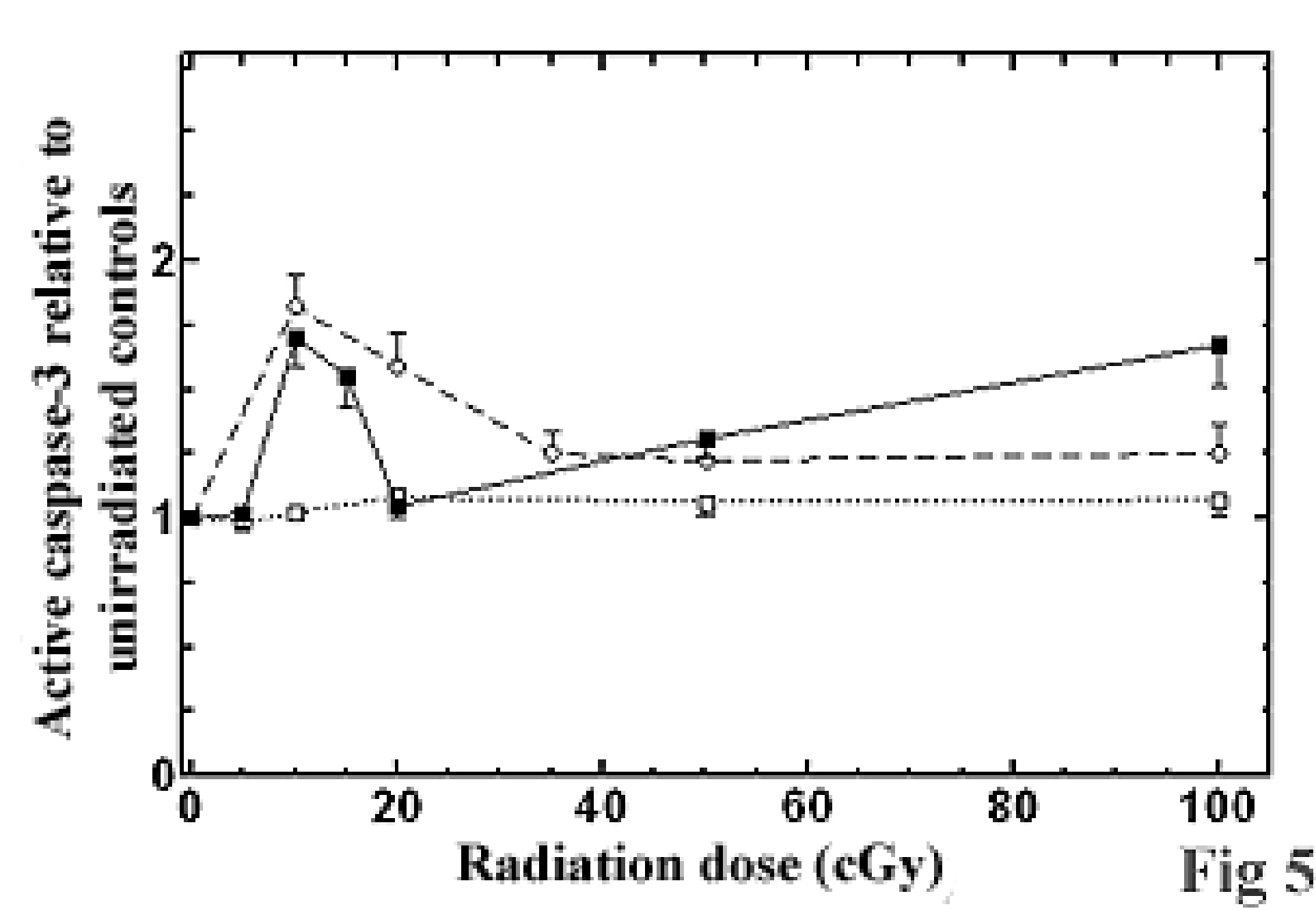
Active caspase-3 relative to unirradiated controls
0
1
2
0
20
40
60
80
100
Radiation dose (cGy)

Fig 5

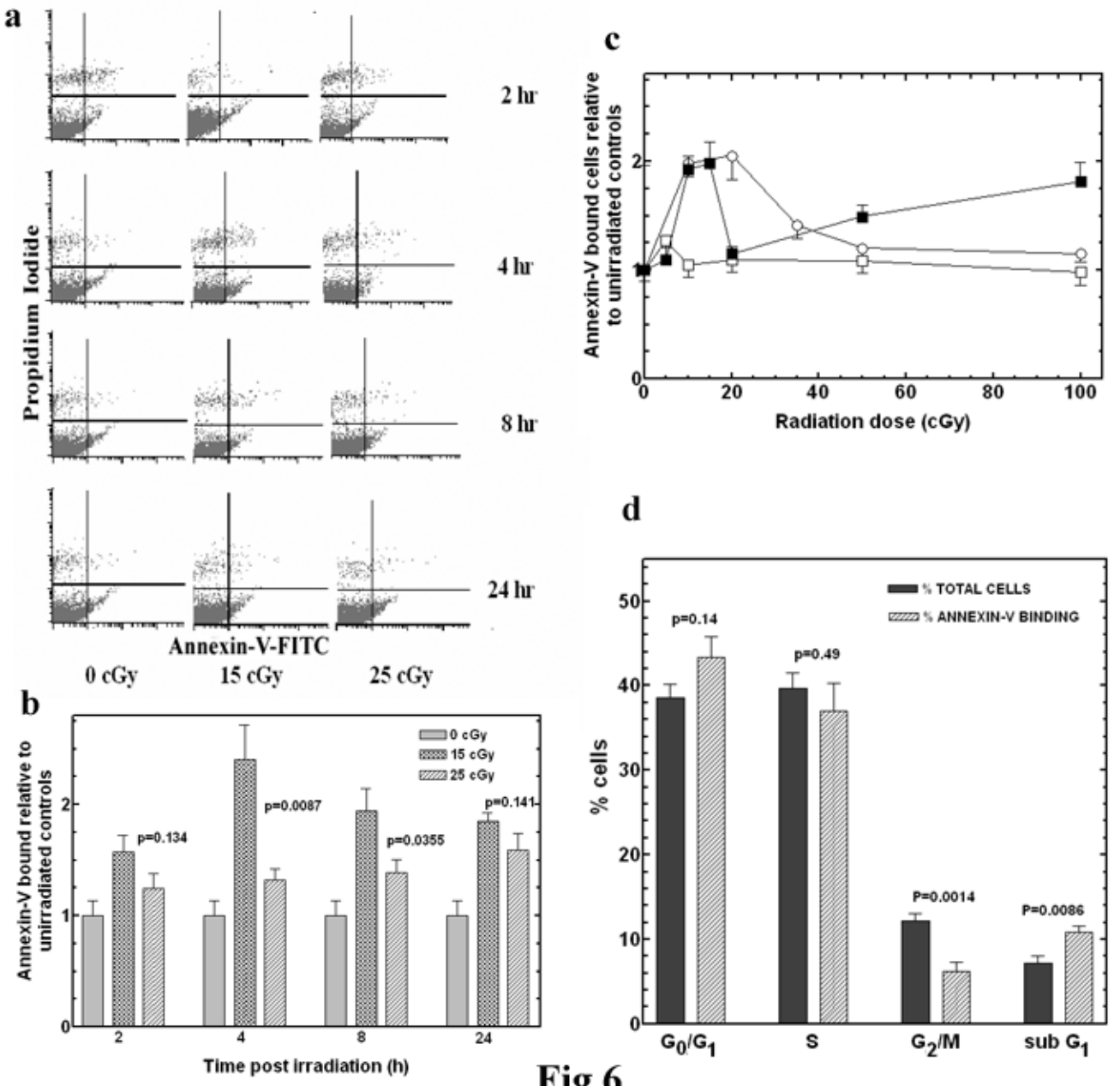
a
2 hr
4 hr
8 hr
24 hr
Propidium Iodide
Annexin-V-FITC
0 cGy
15 cGy
25 cGy
b
Annexin-V bound relative to unirradiated controls
0 cGy
15 cGy
25 cGy
p=0.134
p=0.0087
p=0.0355
p=0.141
Time post irradiation (h)
c
Annexin-V bound cells relative to unirradiated controls
Radiation dose (cGy)
d
% cells
% TOTAL CELLS
% ANNEXIN-V BINDING
p=0.14
p=0.49
P=0.0014
P=0.0086
G0/G1
S
G2/M
sub G1

Fig 6

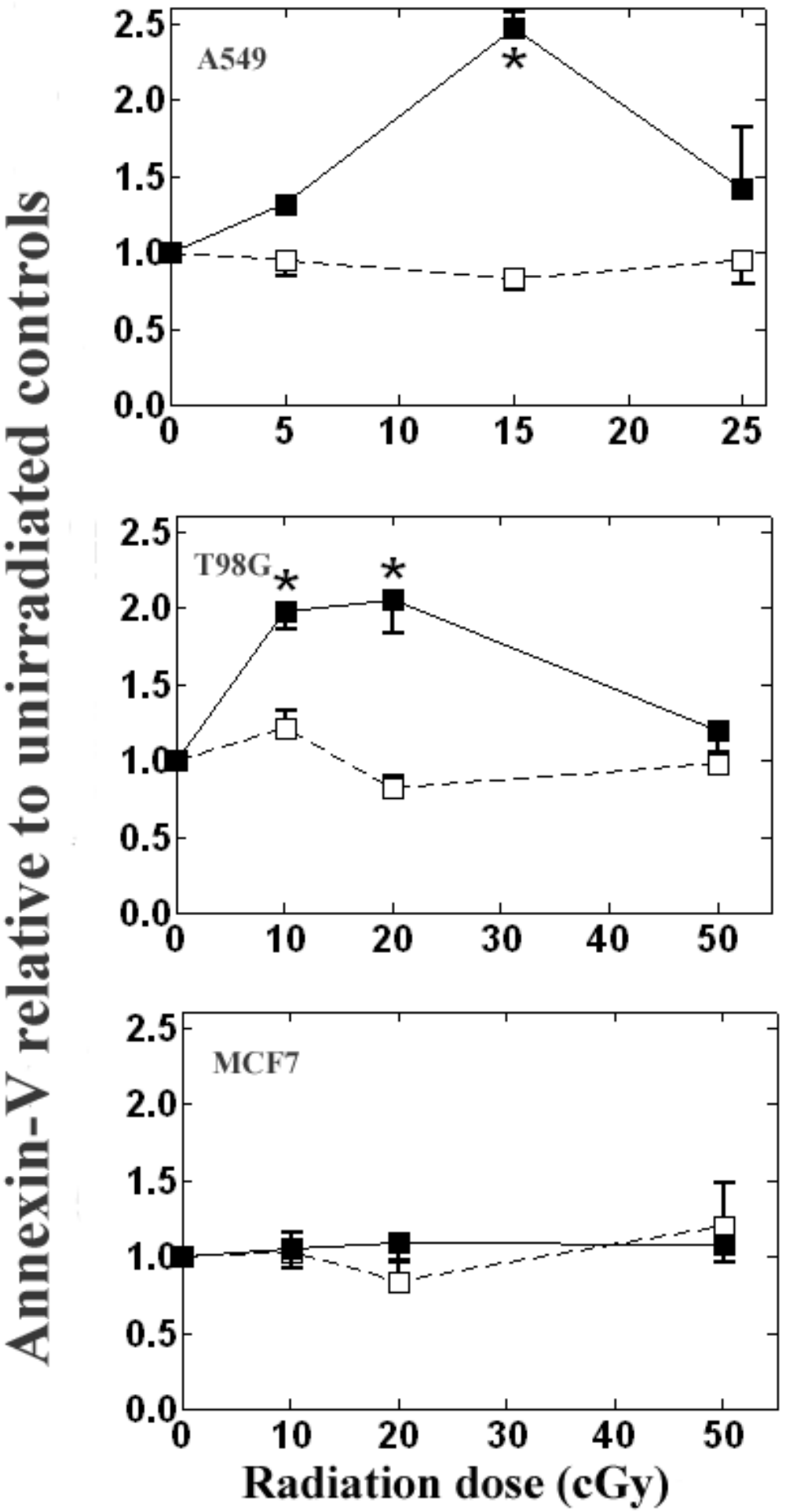
A549
T98G
MCF7
Annexin-V relative to unirradiated controls
Radiation dose (cGy)
0.0
0.5
1.0
1.5
2.0
2.5
0
5
10
15
20
25
30
40
50
*

Fig 7

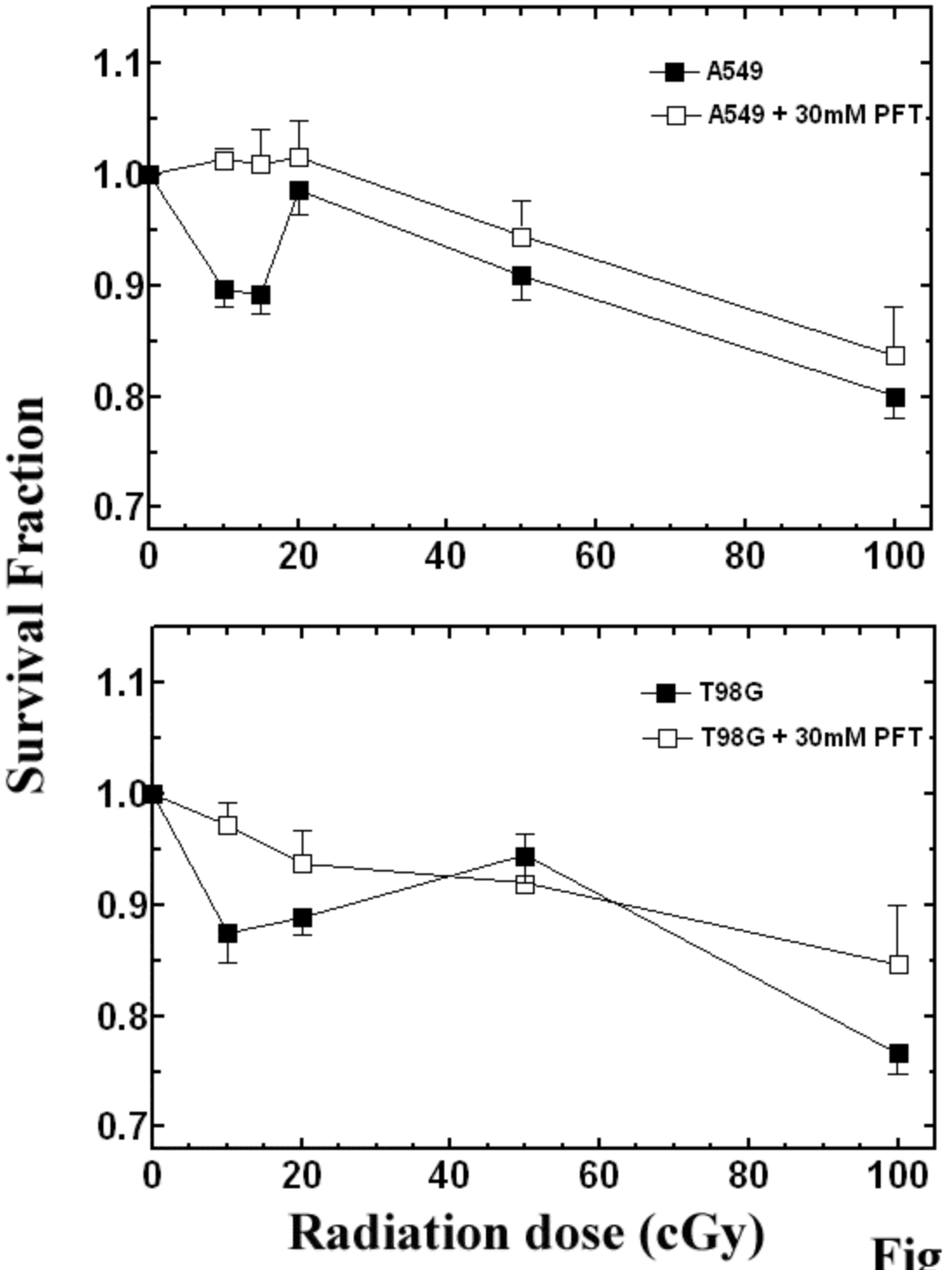
A549
A549 + 30mM PFT
T98G
T98G + 30mM PFT
Survival Fraction
Radiation dose (cGy)
1.1
1.0
0.9
0.8
0.7
0
20
40
60
80
100

Fig 8

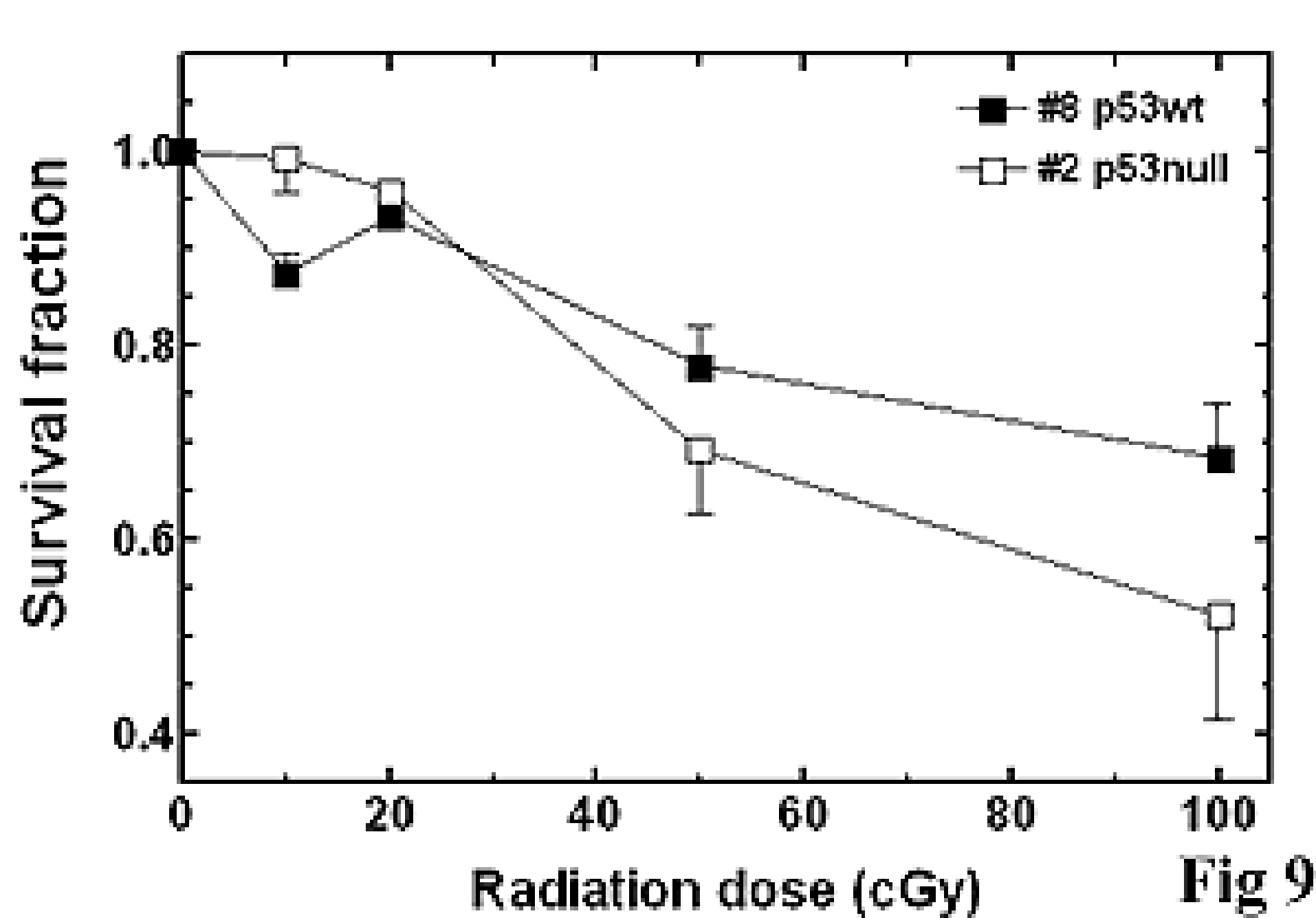
#8 p53wt
#2 p53null
Survival fraction
1.0
0.8
0.6
0.4
0
20
40
60
80
100
Radiation dose (cGy)

Fig 9

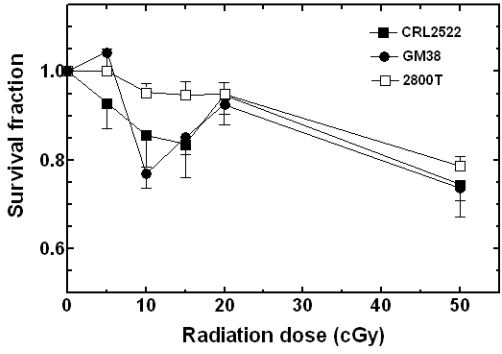
CRL2522
GM38
2800T
Survival fraction
1.0
0.8
0.6
0
10
20
30
40
50
Radiation dose (cGy)

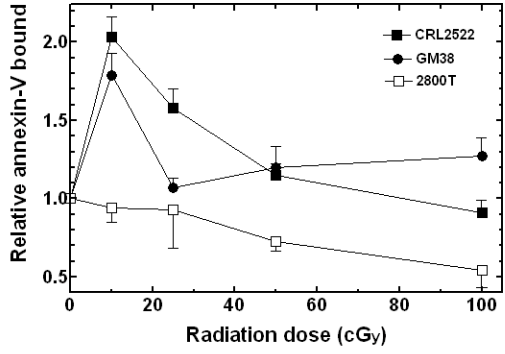
CRL2522
GM38
2800T
Relative annexin-V bound
2.0
1.5
1.0
0.5
0
20
40
60
80
100
Radiation dose (cGy)

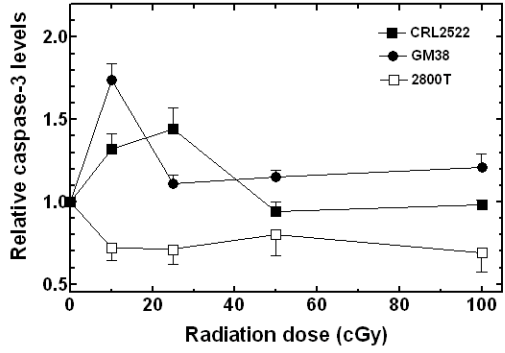
CRL2522
GM38
2800T
Relative caspase-3 levels
2.0
1.5
1.0
0.5
0
20
40
60
80
100
Radiation dose (cGy)

Fig 10